Saudi Journal of Biological Sciences 28 (2021) 1990–1998

Contents lists available at ScienceDirect

Saudi Journal of Biological Sciences

journal homepage: www.sciencedirect.com

Original article

MR image analysis of ex-vivo mouse model of heart ischemia

Faiz Alqarni [a,c], Mohammed Alsaadi [b,*], Fayka Karem [a,d]

[a] Medical Imaging Department, King Saud Medical City, Riyadh 12746, Saudi Arabia
[b] Prince Sattam Bin Abdulaziz University, College of Applied Medical Sciences, Radiology and Medical Imaging Department, PO Box 422, Alkharj 11942, Saudi Arabia
[c] Centre of Advanced Imaging, University of Queensland, Brisbane, St Lucia, QLD 4072, Australia
[d] Al Azhar University, Faculty of Medicine for Girls, Radiology and Medical Imaging Department, P.O Box: 1175,Cario, Egypt

ARTICLE INFO

Article history:
Received 10 July 2020
Revised 28 December 2020
Accepted 29 December 2020
Available online 6 January 2021

Keywords:
Ex-vivo
Mouse model
Myocardial infarction
Cardiac magnetic resonance
Cardiac imaging

ABSTRACT

Introduction: Myocardial infarction is one of the major causes of death and disability. Various diagnostic modalities used to investigate cardiac ischaemia. Advances in Magnetic Resonance Imaging technology has opened up new horizons for investigating the cardiac function and quantifying any pathology that may be present.
Aims: The present study was designed to quantify the cardiac area at risk and infarction reperfusion areas using the mismatch of iron oxide contrast and gadolinium (Gd) contrast imaging (MRIs) and to test if a combination of T1, T2, and iron oxide T2* contrasts will distinguish the infarction and AAR zones.
Methods: A well-established mouse model was used to induced cardiac ischaemia and reperfusion. Six mice models' hearts were harvested and processed according to various protocols. MI was induced through ligation technique for five mice, and one was kept as normal control. MR imaging and Reperfusion were performed using a Three-dimensional gradient-echo fast low angle shot (3DFLASH) and three-dimensional multi-slice multi-echo sequence (3DMSME). Generation of T1 and T2 maps, image post-processing including segmentation and mismatch measurement and drawing of the area of interest.
Results: The edematous myocardium had significant high signal intensity in 3DMSME with variable echo time (14, 28, 42 ms). The combination of 3DFLASH and 3DMSME at an echo time of 42 ms was statistically significant, detecting the AAR more accurately. Both T1 and T2 sequences had the potential to determine the AAR zone. The infarct area has significantly high signal intensity compared to normal areas ($p = 0.04$ for the T1 map and $p = 0.01$ for the T2 map).
Conclusions: The study demonstrated that Cardiac MRI was a valuable technology to investigate infarct areas and zones that are at risk.

1. Introduction

Cardiovascular diseases (CVDs) are the first cause of death worldwide resulting in more than 17 million estimated deaths related to CVDs (WHO). Sudden death is a devastating complication of myocardial infarction (MI) (Huikuri et al., 2001). Death usually occurs in the first few hours after MI due to ventricular dysrhythmia (Henkel et al., 2006; Khairy et al., 2003). Post-MI heart failure and arrhythmias usually arise secondary to overwhelming cardiac sympathetic nerve activity (CSNA) which appears within the first hour of the primary infarction and can sustain for days (Jardine et al., 2005; Shirai et al., 2015). Patients with acute MI usually develop acute myocardial ischemia–reperfusion injury (IRI), causing additional injury/further cardiomyocyte death. Reducing acute myocardial ischemic injury and limiting the size of MI depends mainly on timely and effective myocardial reperfusion in those patients (Braunwald and Kloner, 1985; Piper et al., 1998; Yellon and Hausenloy, 2007). The IRI can be demonstrated clinically as myocardial arrhythmia, myocardial stunning, and endothelial dysfunction (Hausenloy and Yellon, 2013; Grieve et al., 2014). Despite the availability of various diagnostic tests for MI, they all have some limitations (Friedrich, 2010). Magnetic resonance imaging (MRI) can provide high spatial resolution, which is an excellent

* Corresponding author at: Radiology and Medical Imaging Department, College of Applied Medical Science, Prince Sattam Bin Abdulaziz University, PO Box 422, Alkharj 11942, Saudi Arabia.
E-mail addresses: F.alqarni@ksmc.med.sa (F. Alqarni), m.alsaadi@psau.edu.sa (M. Alsaadi), Fayka@ksmc.med.sa (F. Karem).
Peer review under responsibility of King Saud University.

Production and hosting by Elsevier

https://doi.org/10.1016/j.sjbs.2020.12.054
1319-562X/

tool in discriminating the soft tissue. Cardiac magnetic resonance (CMR) can provide accurate data and offers several theoretical and practical advantages over stress echo and nuclear perfusion. It provides an ideal tool to investigate wall motion and wall thickness in response to stress due to its ability to provide better temporal and spatial resolution to nuclear imaging without the limitations associated with poor echo windows (Daly and Kwong, 2013), in addition to a more quantitative approach for analysis of wall motion by using tissue tagging (Kuijpers et al., 2003).

The cardiovascular disease in mice model has provided an excellent opportunity to study the physiological and molecular mechanisms. The new therapeutic strategies are evaluated by measuring the infarction extent, which leads to quantifying the result more accurately. The standard gold method used to quantify the area at risk (AAR) and the grade of completed infarction are by perfusing the heart with Evans blue and triphenyl tetrazolium chloride (TTC) to stain the post-mortem sectioned heart. In this method, the heart is sliced manually; the slices are thicker. The lack of outlining of the border of the AAR and the infarct regions will be subject to the assumption of the actual boundary of the ischemia–reperfusion (IR) and AAR regions. Moreover, this method is subjected to the anatomical supply of the coronary artery, which would help the examiner measure the amount of saved myocardium (Grieve et al., 2014). However, Cardiac magnetic resonance (CMR) needs a skilled team to adjust respiratory and cardiac gating when applied on a mouse model.

This study aimed to test the MRI's ability to quickly and accurately quantify the AAR and IR regions using the mismatch of iron oxide contrast and gadolinium (Gd) contrast of magnetic resonance images (MRIs) compared to the gold standard method. We hypothesize that a combination of T1, T2, and iron oxide T2* contrasts will distinguish the infarction and AAR zones.

2. Methods

2.1. The animal and experimental model of myocardial injury

Six mice C57BL6 models were adapted for one week before the surgery. The procedure was conducted under protocols approved by the University of Queensland and used for imaging at the Centre of Advanced Imaging (CAI).

Five mice underwent open-chest surgery, ligation of the left anterior coronary artery for 30 min using a transient suture to induce myocardial injury and ischemia. The suture location was 2–3 mm distal to the left arterial appendage and the pulmonary artery junction. Then, the suture was removed, and the mice were kept for recovery for 48 h. The sixth mouse was normal and used as a control for MRI imaging. All mice were kept in continuous anaesthesia and injected with gadopentetate dimeglumine 0.15 mmol/kg through the tail vein. Then, 10 min later, the heart was infused with a solution containing mixed Evans blue stain and MPIO. Two minutes later, the mice's hearts were harvested and placed for 20 min at 37 °C in phosphate-buffered saline. Mice Hearts were placed in agar gel and stored at 4 °C (Fig. 1), to reduce the slicing movement during MRI, (Grieve et al., 2014).

2.2. Magnetic resonance imaging protocols

2.2.1. Sample preparation for MRI imaging

All the six samples were examined by using a vertical 16.4 T magnet (Biospec, Bruker, Ettilingen, Germany). Each heart (H) was given number, and the samples were prepared into two groups with three hearts each time, so in the first group, the hearts were placed on the magnet bed in order from bottom to top as H1, H2, H3. Heart1 (H1) was normal and was used only as a control, while the remaining two hearts (H2, H3) were injured. The second sample group comprised three hearts and was organized in the same order from bottom to top, H4, H5, H6, and all three of the hearts in group 2 were injured; the injury size and location in both samples were different.

2.3. MRI sequences

2.3.1. Three-dimensional (3D) gradient-echo fast low angle shot (FLASH)

Imaging parameters of Three-dimensional (3D) gradient-echo (GE) fast low angle shot (FLASH) were as following: [echo time (TE) 6.735 ms, repetition time 40 ms, the number of averages is two and the scan time 39 m, 26 s and 720 ms, the flip angle 30, slice thickness of 10 mm, the spatial resolution 0.040 × 0.039 × 0.039 mm/voxel with the field of view (FOV) 25.600 mm × 10 mm × 10 mm, matrix size of 640 × 256 × 256]. This technique has short scanning time with optimal high resolution. The image contrast in this sequence is a more T2*-weighted image, which helps detect the perfused area from the non-perfused area using microparticles contrast (MPIO) as the signal is lost at the perfused area. The image contrast allowed visualization of the area at risk (AAR) (Fig. 1).

2.3.2. Three-dimensional multi-slice multi-echo sequence

The second sequence was three-dimensional multi-slice multi-echo sequence (3DMSME). The imaging parameters are [multi echo time (TE) 14, 28, 42 ms, the repetition time (TR) 400 ms, the spatial resolution 0.078 × 0.078 × 0.078 mm/voxel, the scanning time took 49 m and 18 s and 400 ms with a slice thickness of 10 mm and FOV of 25.600 × 10 × 10 mm, the matrix size 328 × 128 × 128, the number of averaging 1]. The image contrast is heavily T2 weighted, used for anatomical assessment of the AAR and injured zones (Fig. 2).

2.3.3. T1 map and T2 map

The T1 map was generated to draw the region of interest at the normal area and the infarcted area to measure the signal intensities in both areas. It was generated from the inversion recovery with variable inversion time TI at a range of (300–500-700–800-1000–1500). The repetition time was 4000 ms, while the number of averaging is 1. The spatial resolution was 0.078 × 0.078 mm/voxel with the field of view of 10 × 10 mm. The matrix size is 128 × 128, and the slice thickness is 0.5 mm (Fig. 3).

The T2 was designed from the spin-echo multi-echo sequence with variable echo time TE at a range of (11–22-33–44-55–66-77–88 ms). The repetition time was 5000 ms with a scanning time of 10 m and 40 s. The number of averaging was 1 with FOV 10 × 10 mm and a matrix size 128 × 128 mm. The slice thickness was acquired at 0.5 mm, and the spatial resolution was 0.078 × 0.078 mm/pixel. The injury appears on the T2 map as hyperintense compared to the T1 map (Fig. 4). The T2 map was generated to draw a region of interest at the infarcted area and the normal area to measure the signal intensity in both areas.

2.4. Image post-processing

2.4.1. Image segmentation of 3DFLASH and 3DMSME sequences

Both sequences have different image contrast, so the normal and injured areas will have a different appearance. The segmentation was performed using ITK-SNAP software to colour the normal and infarcted area in 3D. The normal area was coloured with blue, and the infarcted area was coloured with red. The segmentation was acquired manually, and the areas were coloured slice-by-slice in different orientations (axial-coronal and sagittal) to achieve an accurate segmentation for both areas.

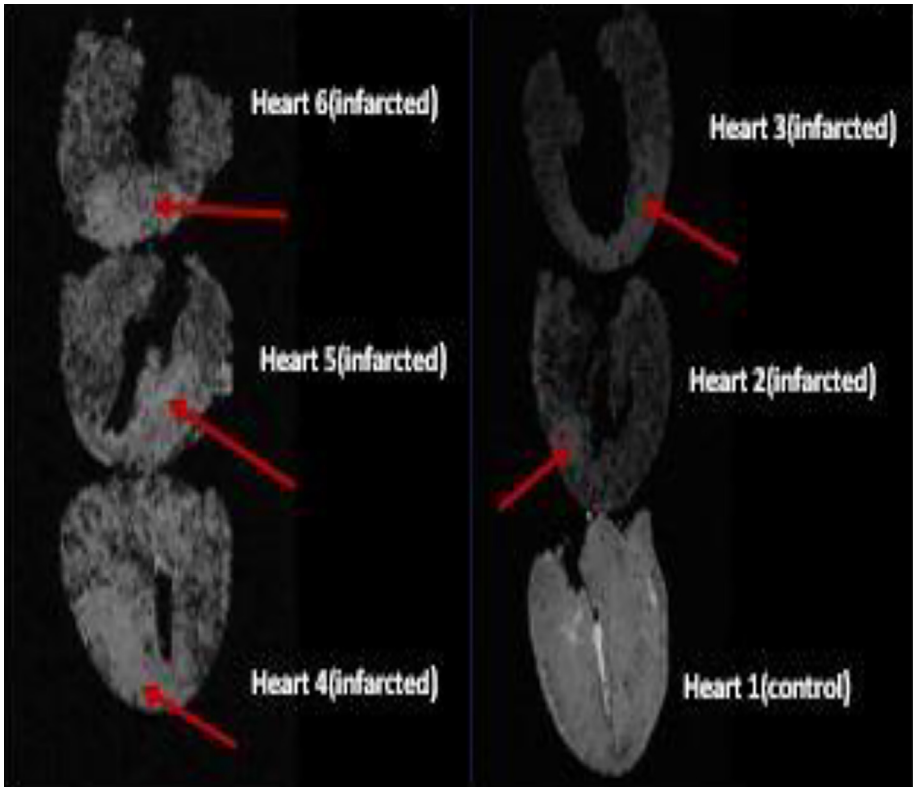

Fig. 1. 3DFLASH sequence for the six samples. Infarcted area is shown (red arrow).

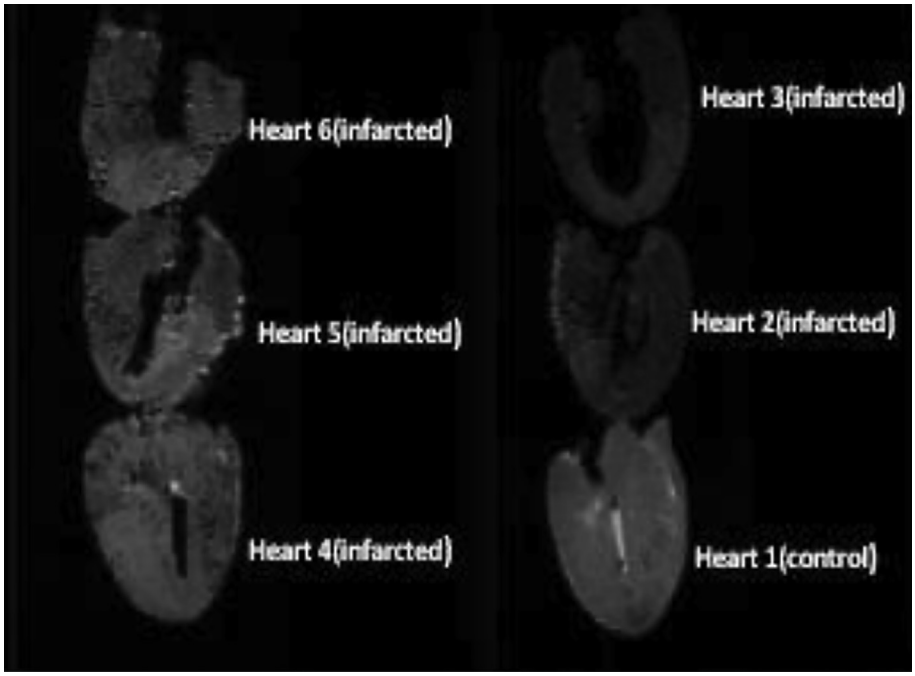

Fig. 2. 3DMSME image of the six samples with TE of 42 ms.

The image assessment and definition of the normal area from the infarcted area were based on a visual inspection. The infarction appears in 3DFLASH sequence as a non-perfused area, while in 3DMSME as a hyperintense area. This process was applied to compare the injured area's size between the two sequences, as each sequence has a different sensitivity to the injured area (Fig. 5). After the segmentation was completed, the voxel volume was measured for both normal and injured areas using the statistical volume from ITK-SNAP. All the voxel measurements were extracted and used for an Excel spreadsheet to measure the differences between normal and injured areas and between sequences.

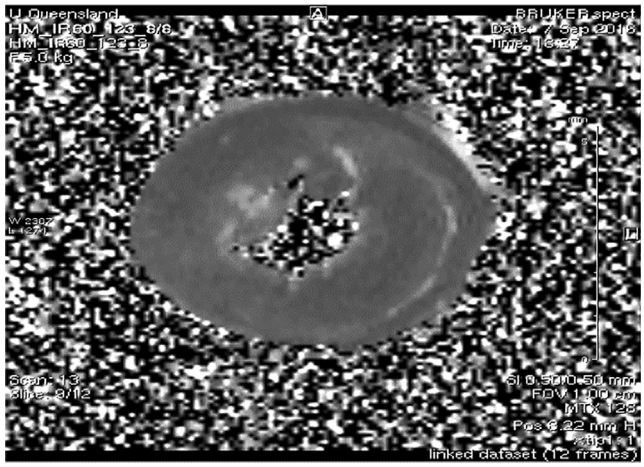

Fig. 3. An axial slice of the T1 map image.

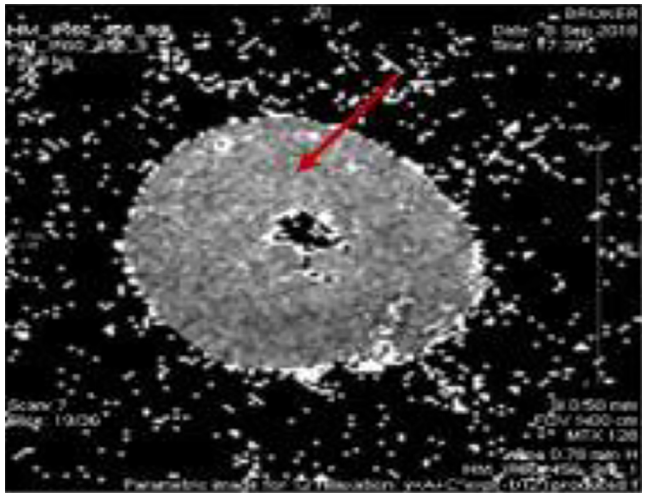

Fig. 4. An axial slice of T2 map with hyperintensity at the infarcted zone (red arrow).

2.5. Mismatch area measurement

The mismatch area is the area that appears different when you subtract different sequences from each other. In other words, the mismatch area is considered the area at risk (AAR), which is related to the infarcted area and to the normal area. The process started after the segmentation was completed as the normal and injured areas were delineated. FSL software was used to subtract different sequences from each other by using the following command (fslmaths 3DMSMETE42- sub 3DMSMETE28 mismatch42-28.nii).

The first sequence used is the 3DMSME as it has a different echo time TE (42.28 and 14 ms), which has different contrast and a different size of the infarcted area. The same image subtraction process was applied on the 3DFLASH sequence. Before subtracting 3DFLASH from 3DMSME, the 3DFLASH had to be normalized and oriented to the same orientation as the 3DMSME using FSL linear registration software (FLIRT). As a result, we had an image that could be subtracted from 3DMSME at different echo time TE. After the subtraction was completed, we had an image with three areas that identified as normal, infarcted, and the mismatch area was the AAR (Fig. 6). Finally, all the voxel volume was extracted for each area and used in an Excel spreadsheet to calculate the normal, infarcted and mismatch areas.

This cross-section 3D image shows how our automated approach precisely detects the nature of AAR, MI and the normal zones. This view shows the clear outlining of all the zone borders. As a result, this will help the examiner scroll through the image to identify the zones' anatomical relationship.

2.6. T1 map and T2 map ROI, s selection

The region of interest (ROI) was drawn using Paravision software 5.1. Before that, we had to generate a T1 and T2 map. The T2 map was generated from a spin echo-multi echo sequence with echo time (11, 22, 33, 44, 55, 66, 77, 88 ms). Then, the image contrast was adjusted, and a coloured threshold was added to achieve a good image contrast for visual assessment. The injured area on T2 was detected visually as it holds high T2 value and appears hyperintense. The ROI was drawn based on the appearance of the injured area and another RIO was drawn on the normal area. Then, the T2 value with the standard deviation of each area was extracted, and entered in the Excel spreadsheet for calculation. The same process was used on the T1 map, which was generated from the inversion recovery sequence with multi TI of (300, 500, 700, 800, 1000, 1500 ms). The visual assessment on the T1 map was a bit difficult as it was hard to distinguish between the injured and normal areas. Therefore, the same ROI drawn on the T2 map was copied and pasted onto the same slice at the same area on the T1 map. Again, the T1 values of the injured and normal areas with the standard deviation were extracted and entered in the Excel spreadsheet for further calculation (Fig. 7).

3. Results

3.1. Analysis for normal, infarcted and mismatch areas

The injury size in each of the five hearts, heart2 (A), heart 3 (B), heart 4 (C), heart 5 (D), and heart 6 (E) was different (Fig. 8). The primary visual assessment of the MRI data, concentrating on the T2* using FLASH sequence with nanoparticles and T2 using the MSME sequence for the five heart samples revealed that signal loss appears as black dots in perfused areas and, absence of black dots at the un-perfused areas in the FLASH sequence. In contrast, oedema appears in the MSME sequence as a high signal and the normal area as a low signal. The quantities measurement of infarcted, normal and the mismatch area (AAR), were also different between the two sequences. In the FLASH sequence and nanoparticles, we can identify the non-perfused area of 8.6%, 19.7%, 26.9%, 7.5%, and 10.3% in the injured hearts 2–6 respectively (A, B, C, D, and E). Moreover, the normal tissue measurement in all hearts was variable at 91.3%, 67%, 26.9%, 92.4%, 89.6% in hearts 2–6 respectively. In the MSME sequence, the results are variable depending on the TE used. In heart 2 the normal tissue ranges from 90.7% to 95% and oedema ranges from 6.6% to 9.7% of the area. In hearts 3 and 4 the normal range was 52.7–69.3%, and 72.2–91% for hearts 5 and 6, while the oedema range was 19.7–30% and 8.9–27.7% respectively. A comparison of the cardiac areas derived from FLASH and MSME shows that the oedema area is typically larger than the non-perfused areas. In general, the longer the echo time (TE), the larger apparent oedema became; however, the overall heart size became smaller, because the longer TE produced lower SNR, such that the apparent heart size is smaller.

Using the sum of both FLASH and MSME, sequences can refine the assignment of the heart tissue type as normal, infarcted core, and AAR (with oedema). Such that the area ranges are 40–90%, 6.4–18.1%, 2.9–8%, respectively. Tests for statistical significance included the one-tailed, one type *t*-test for different TE (14, 28, 42 ms), where >0.05 P- is considered significant. The P-value of

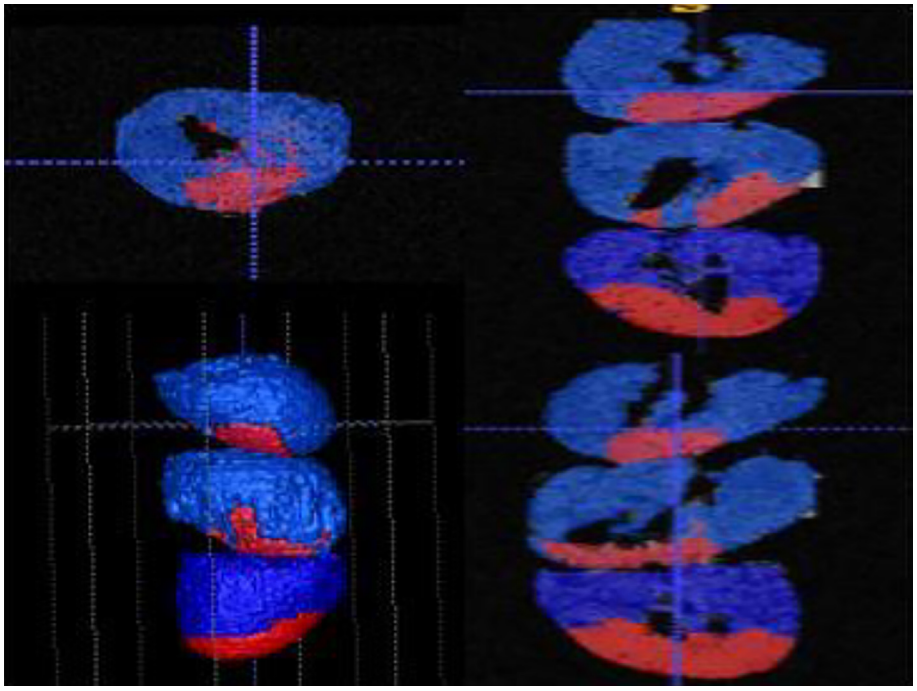

Fig. 5. Image segmentation of three infarcted hearts coded with red and the normal tissue coded with blue of 3DFLASH sequence.

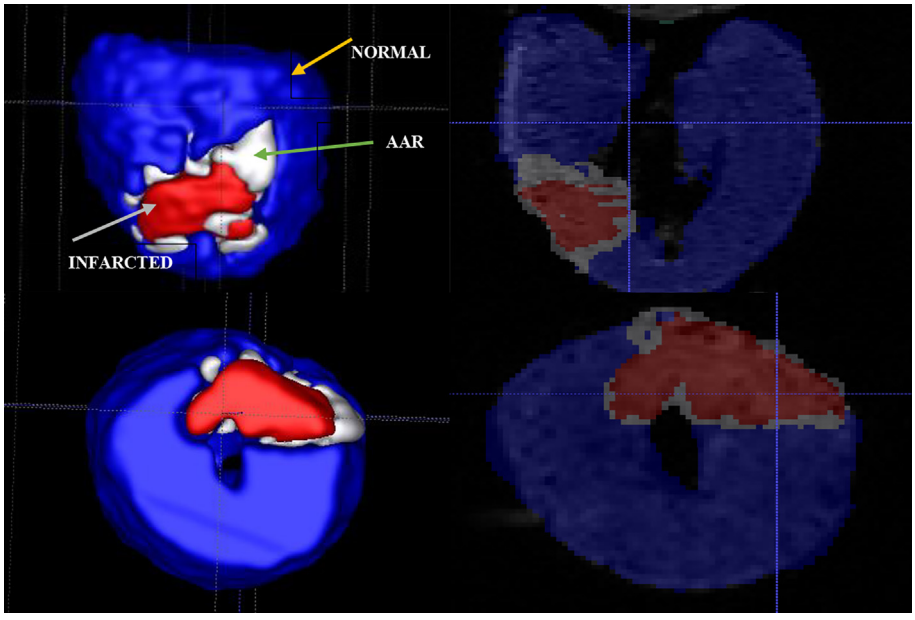

Fig. 6. 3D reformats of a whole mouse heart after subtraction 3DFLASH from 3DMSME – TE 42 ms. The normal area is coded as blue, the infarct area as red and the AAR as white.

TE of 42 ms is 0.03, while the other echo times did not show statistical significance. As a result, in this study, the combination of FLASH and MSME at TE 42 ms is more optimal than other echo times as it shows significant results.

3.2. Effect of echo time in 3D-multi slice multi-echo

Using multi-echo time in the 3DMSME sequence has a variable signal intensity depending on the echo time length. As mentioned earlier, the longer the TE, the less SNR is produced. Thus, each heart has a different infarct volume at other echo times (Fig. 9). The infarct volume for heart 2 was large at TE 14 ms, while for hearts 4 and 5 at TE 28 ms. Therefore, it is difficult to conclude that the volume of MSME infarct was influenced by the echo time. Instead, this variability shown in Fig. 9 may be due to variability in tissue fixation, which may change oedema (water tissue) content in ex-vivo samples compared to the living tissues.

3.3. The image analysis for T1 and T2 maps

In both sequences in the T2 map, the infarction area's signal intensity was more significant than the normal area. The *t*-test cal-

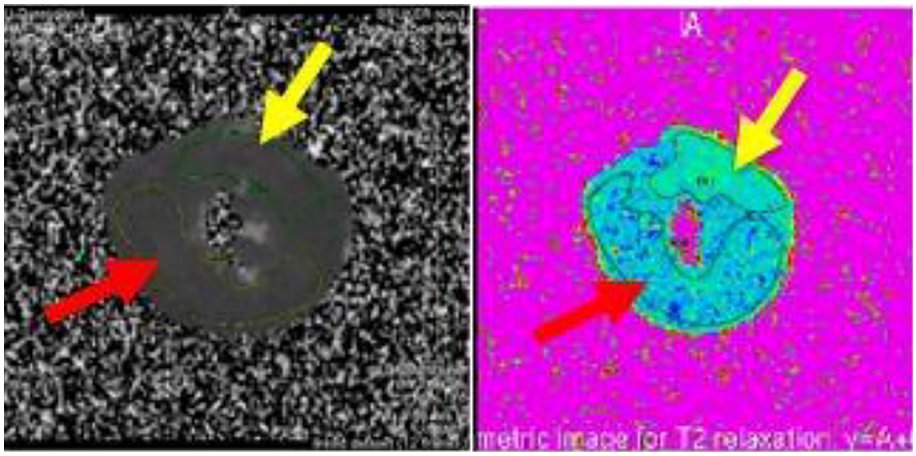

Fig. 7. T1 map (left) and T2 map (right) with drawing ROI (yellow arrow) for infarcted area and ROI (red arrow) for the normal area.

culation was used to determine any statistical significance in both the T1 and T2 maps (Fig. 10). As a result, the P-value was 0.001 for the T2 map and 0.04 for the T1 map, which indicates both are significant in determining the normal from the infarcted tissue. In the T1 map, the infarcted area's signal intensity should be low as the Gd bind with the infarcted area. However, the Gd did not bind to the infracted site, because the samples had died before the iron was given as it has the same incubation with Gd. Moreover, the samples have some difficulties with suture placement, which may have iron throughout the whole heart.

4. Discussion

A combination of T1, T2, and T2* was acquired using 3DFLASH, 3DMSME, and 2D spin-echo sequences for six post-mortem hearts of a mouse model. The experiment was conducted using an ultra-high field of 16.4 T to assess the heart tissue, resulting in identifying the myocardial infarction size (MI) and area at risk (AAR).

The current study was conducted on an ex-vivo mouse model which provides an excellent procedure to study the heart, as in-vivo mouse model imaging is challenging and has some difficulties due to the rapid movement of the heart and heart gating (Beyers et al., 2012).

Bayers and his group (2012) designed a T2 technique, which provides a high signal intensity from the myocardium oedema. They reported that using the prep T2 of echo time at 60 ms offers high contrast between normal and oedematous tissue. Moreover, the AAR was 33% of the left ventricle mass LV in T2-weighted and 15% in T1-weighted, both resemble the histology measurement. In their study, the MI size was smaller than the AAR for all samples, so the salvaged area was 50% of the AAR. They were able to assess 20–50% of the left ventricular mass. Beyers et al. (2012) method could be useful in evaluating the salvaged area after MI. However, the therapy and preconditioning of the ischemic area could affect the signal intensity of T2 and the water content, individually of the real AAR. Thus, in-vivo assessment of MI and the AAR using CMRI is technically challenging and less accurate than high-resolution ex-vivo imaging.

Our study found that the injury size and percentage were different in 3DMSME depending on the echo time due to the nature of the injury at each sample and the chemical exchange in each sample as it is ex-vivo, which is different from live tissue. This high variability in the infarct and normal areas in different samples could be attributed to the effect of myocardial surgery and not due to MRI. The model used in this study (ischemia/reperfusion MI model) could provide more clinically relevant results than those obtained using a permanent occlusion model (Hashmi and Al-Salam, 2015).

We induced MI through ligation of the LCA for 30 min. Ligation is the most common technique to cause myocardial injury, and 30 min is the most common time used in previous studies. Even if the LCA was closed at what seems to be the same area for every mouse, the difference in the anatomy of the coronary artery and myocardium zone supplied by vessels would result in differences of the AAR. Including the AAR measurement will lead to assessing the MI size concerning AAR, and the result of treatment on the salvaged area to be fully valued.

In this study, we experienced a user-friendly technique using MRI to identify the AAR border using MPIO instead of Evans blue. While the MI area can be identified using the late enhancement Gd, MRI provides digital data with high resolution and replaces the manual slicing of the post-mortem heart with a manual segmentation on the digital dataset. MRI has a significant advantage because, through image analysis of the whole heart, the user can scroll through slices to assess the anatomical relationships between different areas and quantify the tissue through automated segmentation. A previous study reported that the 3D high-resolution MRI would allow the examiner to evaluate the myocardium's internal structure instead of the surface, which will improve the measurement of the affected area and less intra-observer variability (Grieve et al., 2014).

The quantitative measurement using MRI for the AAR shows significant results in this study. The 3DMSME with variable echo time (14, 28, 42 ms) shows high signal intensity in the oedematous myocardium. The combination of 3DFLASH and 3DMSME at TE 42 ms was statistically significant, which can detect the AAR more accurately and more easy analysis for the investigator to analyze the affected area and the relationship between the tissues.

In this study, we acquired T1 and T2 maps to calculate the infarcted and normal areas' signal intensity. In both sequences, the infarcted zone has significantly high signal intensity compared to the normal area ($p = 0.04$ for the T1 map and $p = 0.01$ for the T2 map). Hence, both the T1 and T2 maps have shown the potential to determine the AAR zone.

Previous studies on animals and humans revealed that MRI could accurately assess the infarct size and cardiac function (Yang et al., 2004; Kim et al., 1996; Rochitte et al., 1998; Rogers et al., 1999; Kim et al., 2000). Park et al. (2017) concluded that MRI could provide information about inflammatory responses and disease progression in a mouse model of acute MI.

This study's strengths include it abolished the need for gold standard technique involving physical slicing of the heart tissue and

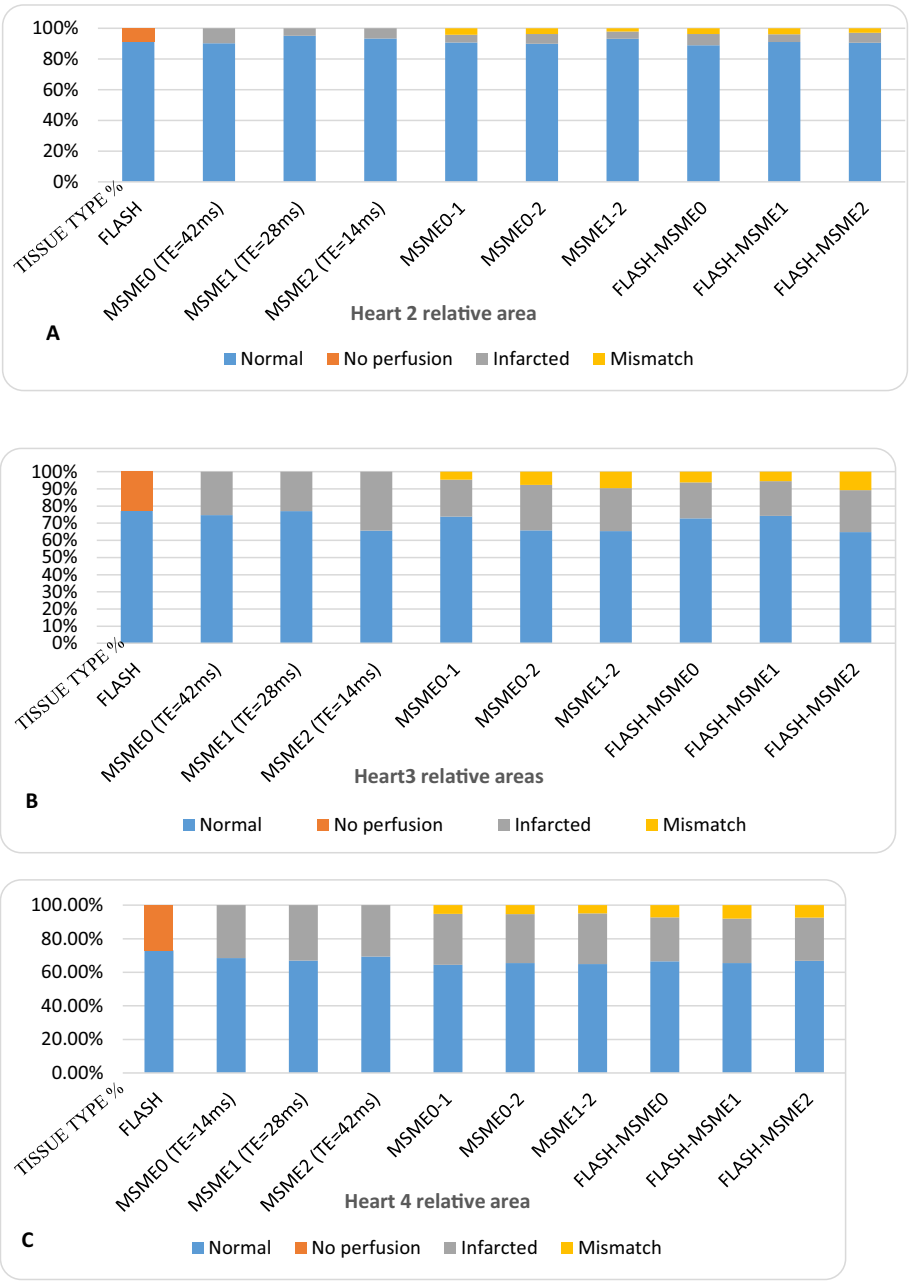

Fig. 8. Percentages of the normal, infarcted and mismatch areas of the 5 injured hearts.

provides the chance of 3D automated digital analysis with a high-resolution MR image. The use of animal models offers an excellent opportunity to understand the nature of the pathology. Mice models are not expensive, and cardiac surgery can be easily performed. This ex-vivo tissue study has solved heart movement and the challenge of engendering to image a mouse heart, which has a high heart rate compared to the human heart (Grieve et al., 2014).

This study has some technical limitations which include: the assessment of the infarcted and normal areas was based on visual judgment, which is different among individuals, the image segmentation was performed manually, which has some inherent error at the heart border and between normal and injured tissue, the samples have some artefacts during the surgery, which result in difficulty distinguishing whether normal or injured.

Future studies are warranted using different techniques and injury time and in-vivo to have more data on the usefulness of MRI in the cardiac imaging field.

5. Conclusion

This study showed that high-resolution CMRI could provide a quantitative measurement of the injury size and the salvaged area. Besides, CMRI had reliable results compared to the histology technique to determine the injured, normal, and area at risk. The use of the 3DFLASH sequence along with MPIO, significantly differentiates the perfused from the non-perfused area. Moreover, the injury size and percentage are different in 3DMSME depending on the echo time, which reflect the nature of the injury at each sample and the chemical exchange in each sample. Hence, both T1 and T2 maps showed significant results and both are reliable in distinguishing between the normal and infarcted areas. Future studies are warranted on a large sample and including different image processing techniques to evaluate whole cardiac function and estimate pathology.

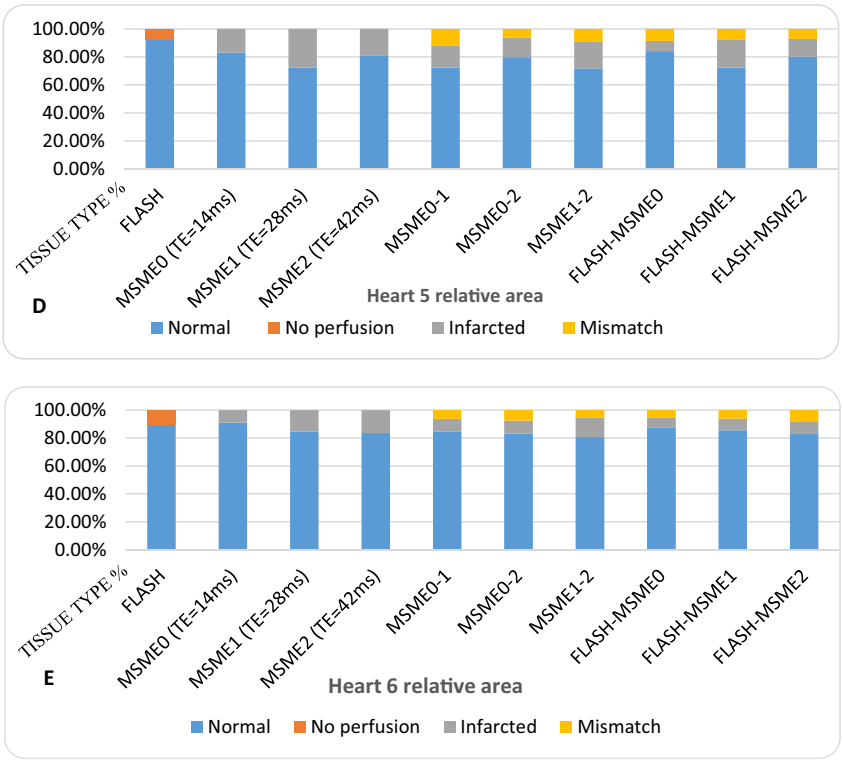

Fig. 8 (*continued*)

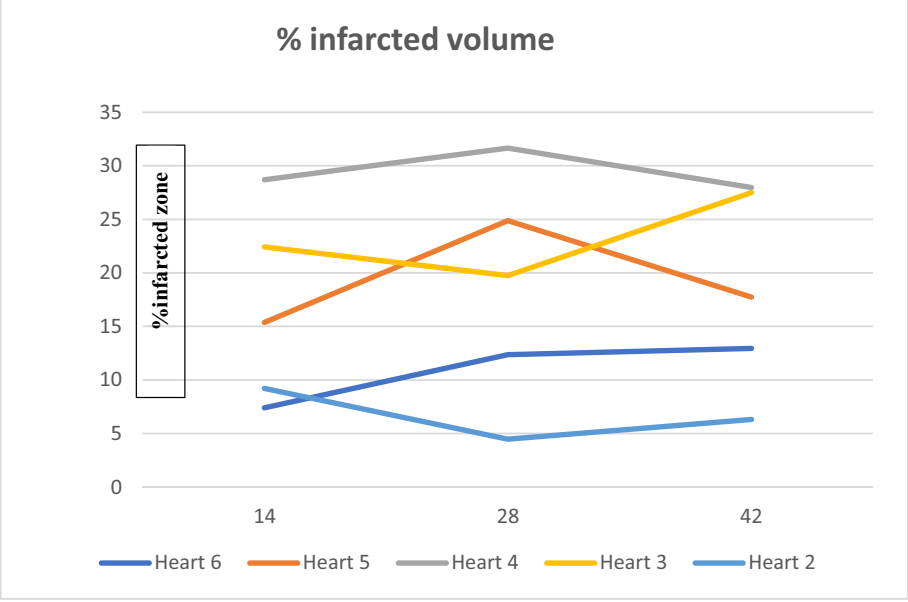

Fig. 9. Percentage of infarcted volume of infarcted area in each heart at different echo time (TE): 14, 28, 42 ms.

Declaration of Competing Interest

The authors declare that they have no known competing financial interests or personal relationships that could have appeared to influence the work reported in this paper.

Acknowledgments

This project was supported by the deanship of scientific research at Prince Sattam bin Abdulaziz University. Also, the author acknowledges the contribution of Hayley MacDonald, Nyo-

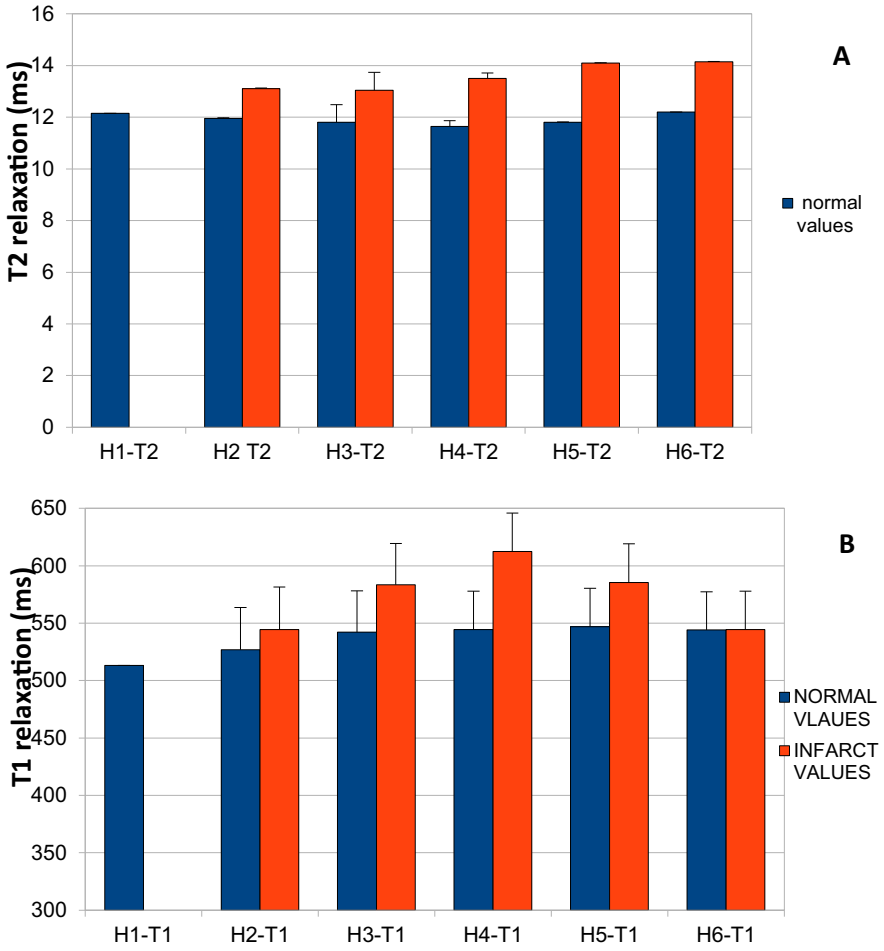

Fig. 10. The differences in signal intensity between normal and infarcted tissue at T1 map (A) and T1 map (B).

man Kurniawan and Chen Chen for the provision of the MRI data, and support from NIF and NCRIS for the operation of 16.4 T MRI at the University of Queensland. The author also appreciates the support of King Saud Medical City- Riyadh for the scholarship.

References

Beyers, R.J., Smith, R.S., Xu, Y., Piras, B.A., Salerno, M., Berr, S.S., Meyer, C.H., Kramer, C.M., French, B.A., Epstein, F.H., 2012. T2-weighted MRI of post-infarct myocardial edema in mice. Magn. Reson. Med. 67 (1), 201–209.

Braunwald, E., Kloner, R.A., 1985. Myocardial reperfusion: a double-edged sword?. J. Clin. Invest. 76 (5), 1713–1719. https://doi.org/10.1172/JCI112160.

Daly, C., Kwong, R.Y., 2013. Cardiac MRI for myocardial ischemia. Methodist DeBakey Cardiovasc. J. 9 (3), 123.

Friedrich, M.G., 2010. Testing for myocardial ischemia: the end of surrogates?. J. Am. Coll. Cardiol. Img. 3 (4), 385–387.

Grieve, S.M., Mazhar, J., Callaghan, F., Kok, C.Y., Tandy, S., Bhindi, R., Figtree, G.A., 2014. Automated quantification of myocardial salvage in a rat model of ischemia-reperfusion injury using 3D high-resolution magnetic resonance imaging (MRI). J. Am. Heart Assoc. 3, (4) e000956.

Hashmi, S., Al-Salam, S., 2015. Acute myocardial infarction and myocardial ischemia-reperfusion injury: a comparison. Int. J. Clin. Exp. Path. 8 (8), 8786–8796.

Hausenloy, D.J., Yellon, D.M., 2013. Myocardial ischemia-reperfusion injury: a neglected therapeutic target. J. Clin. Investig. 123 (1), 92–100.

Henkel, D.M., Witt, B.J., Gersh, B.J., Jacobsen, S.J., Weston, S.A., Meverden, R.A., Roger, V.L., 2006. Ventricular arrhythmias after acute myocardial infarction: a 20-year community study. Am. Heart J. 151 (4), 806–812.

Huikuri, H.V., Castellanos, A., Myerburg, R.J., 2001. Sudden death due to cardiac arrhythmias. N. Engl. J. Med. 345 (20), 1473–1482. https://doi.org/10.1016/j.ahj.2005.05.015.

Jardine, D.L., Charles, C.J., Ashton, R.K., Bennett, S.I., Whitehead, M., Frampton, C.M., Nicholls, M.G., 2005. Increased cardiac sympathetic nerve activity following acute myocardial infarction in a sheep model. J. Physiol. 565 (1), 325–333.

Khairy, P., Thibault, B., Talajic, M., Dubuc, M., Roy, D., Guerra, P.G., Nattel, S., 2003. Prognostic significance of ventricular arrhythmias post-myocardial infarction. Canadian J. Cardiol. 19 (12), 1393–1404.

Kim, R.J., Chen, E.L., Lima, J.O., Judd, R.M., 1996. Myocardial Gd-DTPA kinetics determine MRI contrast enhancement and reflect the extent and severity of myocardial injury after acute reperfused infarction. Circulation 94 (12), 3318–3326.

Kim, R.J., Wu, E., Rafael, A., Chen, E.L., Parker, M.A., Simonetti, O., Klocke, F.J., Bonow, R.O., Judd, R.M., 2000. The use of contrast-enhanced magnetic resonance imaging to identify reversible myocardial dysfunction. N. Engl. J. Med. 343 (20), 1445–1453.

Kuijpers, D., Ho, K.Y., van Dijkman, P.R., Vliegenthart, R., Oudkerk, M., 2003. Dobutamine cardiovascular magnetic resonance for the detection of myocardial ischemia with the use of myocardial tagging. Circulation 107 (12), 1592–1597.

Park, C., Park, E.H., Kang, J., Zaheer, J., Lee, H.G., Lee, C.H., Chang, K., Hong, K.S., 2017. MR assessment of acute pathologic process after myocardial infarction in a permanent ligation mouse model: role of magnetic nanoparticle-contrasted MRI. Contrast Media Mol. Imaging 18, 2017.

Piper, H.M., Garcia-Dorado, D., Ovize, M., 1998. A fresh look at reperfusion injury. Cardiovasc Res. 38 (2), 291–300. https://doi.org/10.1016/S0008-6363(98)00033-9.

Rochitte, C.E., Lima, J.A., Bluemke, D.A., Reeder, S.B., McVeigh, E.R., Furuta, T., Becker, L.C., Melin, J.A., 1998. Magnitude and time course of microvascular obstruction and tissue injury after acute myocardial infarction. Circulation 98 (10), 1006–1014.

Rogers Jr, W.J., Kramer, C.M., Geskin, G., Hu, Y.L., Theobald, T.M., Vido, D.A., Petruolo, S., Reichek, N., 1999. Early contrast-enhanced MRI predicts late functional recovery after reperfused myocardial infarction. Circulation 99 (6), 744–750.

Shirai, M., Joe, N., Tsuchimochi, H., Sonobe, T., Schwenke, D.O., 2015. Ghrelin supresses sympathetic hyperexcitation in acute heart failure in male rats: assessing centrally and peripherally mediated pathways. Endocrinology 156 (9). https://doi.org/10.1210/EN.2015-1333.

Yang, Z., Berr, S.S., Gilson, W.D., Toufektsian, M.C., French, B.A., 2004. Simultaneous evaluation of infarct size and cardiac function in intact mice by contrast-enhanced cardiac magnetic resonance imaging reveals contractile dysfunction in noninfarcted regions early after myocardial infarction. Circulation 109 (9), 1161–1167.

Yellon, D.M., Hausenloy, D.J., 2007. Myocardial reperfusion injury. N. Engl. J. Med. 357 (11), 1121–1135. https://doi.org/10.1056/NEJMra071667.